Transactions, **SMiRT-26**
Berlin/Potsdam, Germany, July 10-15, 2022
Division V

Excitation Experiment and Fluid-structure Interaction Analysis on Scale-Model Cylindrical Tank Containing Water

Hiroyuki Yaka[1], Kohei Susukida[2], Yusuke Aoki[2], Masaki Tsuruki[3], Tetsuya Nagata[4], and Motoki Nakane[5]

[1] Researcher, Hitachi, Ltd., 1-1, Omika-cho 7-chome, Hitachi-shi, Ibaraki-ken, 319-1221 Japan (hiroyuki.yaka.yf@hitachi.com)
[2] Engineer, Hitachi-GE Nuclear Energy, Ltd., 2-2, Omika-cho 5-chome, Hitachi-shi, Ibaraki-ken, 319-1221 Japan
[3] Hitachi, Ltd., 1-1 Omika-cho 7-chome, Hitachi-shi, Ibaraki-ken, 319-1221 Japan
[4] Technical Expert, Hitachi-GE Nuclear Energy, Ltd., 2-2, Omika-cho 5-chome, Hitachi-shi, Ibaraki-ken, 319-1221 Japan
[5] Chief Engineer, Hitachi-GE Nuclear Energy, Ltd., 2-2, Omika-cho 5-chome, Hitachi-shi, Ibaraki-ken, 319-1221 Japan

ABSTRACT

During earthquakes, large cylindrical vertical flat-bottomed fixed tanks containing water can undergo "elephant-foot" buckling (EPRI (1990)), which is a design constraint in such tanks. Empirically, the response factor of resonant vibration is reduced due to the damping effect caused by fluid interaction and buckling. The application of "fluid-structure interaction" (hereinafter referred to as "FSI") is expected to incorporate this damping effect and rationalize the evaluation results. The purposes of this study were to search for the modeling conditions in FSI analysis to generate the same buckling behaviour as that in an experiment and to simulate the response acceleration of the experiment accurately.

In the experiment, a parameter study was conducted for the flexibility of the bottom plate that the seismic damage behaviour of low-height tanks may be influenced by the flexibility of the bottom plate. FSI analysis was also conducted for the experimental case where elephant-foot buckling occurred. The results of the analysis showed that elephant-foot buckling occurred at the bottom of the cylindrical tank as in the experiment, and the error in the response acceleration during buckling was only about 6%.

INTRODUCTION

The application of FSI analysis in the seismic evaluation of cylindrical tanks and similar structures is expected to rationalize the design evaluation based on linear analysis. This is because the vibration energy is expected to be dissipated by the fluid-structure interaction effect and by the elasto-plastic deformation associated with buckling.

If the process of buckling due to an earthquake can be simulated, reinforcement work can be minimized even if the seismic hazard is reviewed and strengthened. Furthermore, the actual damage behaviour can be clarified before taking seismic countermeasures, which can contribute to improved safety.

Currently, research is being conducted on buckling analysis of cylindrical tanks with consideration of fluid interaction effects, but the geometry of the tank and the simulation method are limited, and targets of their analysis is not enough to be authorized for design evaluation. Since it is not possible to conduct excitation experiments on large tanks, experiments are conducted on taller, scale-model cylindrical tanks, which are easily subjected to elephant-foot buckling. Also, the fluid-structure coupled vibration of a thin-walled cylindrical tank filled with a liquid such as water is a strongly coupled behaviour, which is difficult

to converge implicitly, so explicit methods have been applied in most of the previous studies (Maekawa (2007)). On the other hand, the simulation method commonly used in dynamic analysis for seismic evaluation is the implicit method.

In the work reported in this paper, an experiment of buckling a tank by the vibration-test-system was conducted and the experiment was simulated by the implicit FSI analysis. In this experiment, the bottom stiffness of the tank was focused on, and it was confirmed that elephant-foot buckling tends to occur in tanks with low bottom stiffness, where the height is approximately equal to the radius, as seen in large tanks. In the analysis, the scaled-down experiment was simulated accurately by FSI analysis with a stabilizing technique on the coupled boundary to prevent divergence of the coupled calculation.

EXCITATION EXPERIMENTS FOR BUCKLING

The tank with a diameter of 300 mm and a wall thickness of 0.3 mm and a height of 200 mm was used to excite the overturning mode with a vibration-test-system while the tank was containing water. Two scale-model cylindrical tanks were prepared, one with low bottom stiffness and the other with high bottom stiffness. The bottom fixation of the one with low bottom stiffness is schematically shown in Figure 1. A stainless-steel circular plate with a thickness of 10 mm was bolted directly to the excitation table at 5 points on the bottom plate. The bottom fixation of the scale-model cylindrical tank with high bottom stiffness is shown schematically in Figure 2. The 20 mm thick aluminium circular plate was bolted to a 15 mm thick stainless steel conversion plate at 24 points on the bottom plate, and the conversion plate was fixed to the excitation table with 20 bolts. Both tanks have a cylindrical body plate made of rolled aluminium sheets with the overlapping portion bonded with epoxy adhesive. The cylindrical body plate and the sides of the circular plates at the top and bottom are bonded with epoxy adhesive.

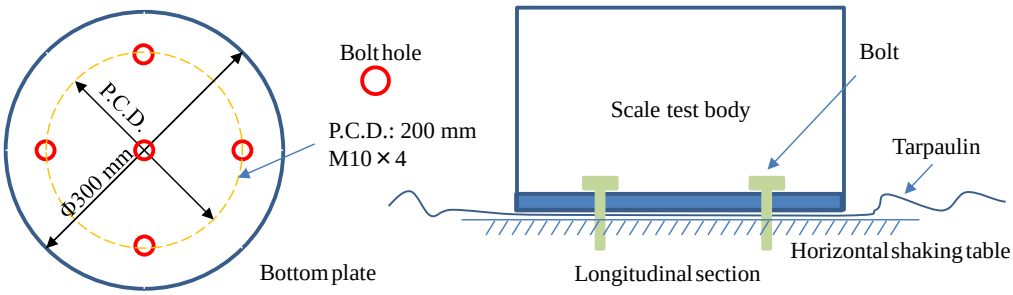

Figure 1 Overview of the scale-model cylindrical tank with low bottom stiffness

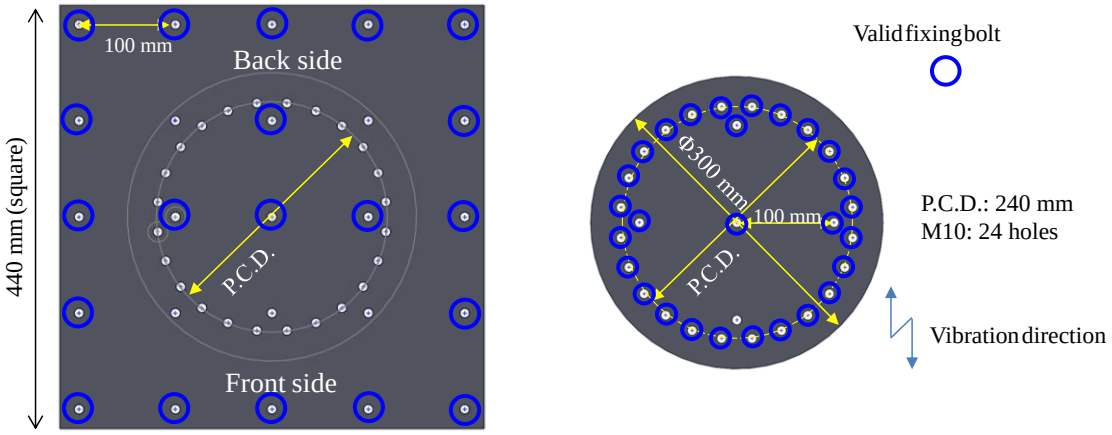

(a) Conversion plate (b) Bottom plate

Figure 2 Overview of jig used for the scale-model cylindrical tank with high bottom stiffness

In the excitation experiments for buckling, the scale-model cylindrical tank was subjected to internal pressure and the bottom plate of the scale-model cylindrical tank was subjected to random excitation acceleration. An electrodynamic vibration-test-system with a horizontal auxiliary table with a maximum force of 40 kN was used for the experiments. Frequency sweep experiments were performed beforehand and the natural frequency of the overturning mode, where the top of the scale-model cylindrical tank vibrates with a high response factor in the direction of excitation, was determined to be about 200 Hz regardless of bottom stiffness. The input acceleration applied to the scale-model cylindrical tank with low bottom stiffness is shown in Figure 3. The PSD of the random waveform used in the buckling excitation experiments is shown in Figure 3(a). The random acceleration waveform with a major component around the natural frequency of 200 Hz in the overturning mode was used as the target input acceleration. The time history waveforms of the input acceleration and the response acceleration at the top of the scale-model cylindrical tank used in the excitation experiments for buckling are shown in Figure 3(b). The amplitude of the input acceleration was gradually increased until the tank started to leak. During the experiments, an air tank was connected to the scale-model cylindrical tank to simulate the hydrostatic pressure near the bottom of the actual tank (70 times larger than the scale-model cylindrical tank), and the internal pressure was maintained at 0.05 MPa during the excitation experiments.

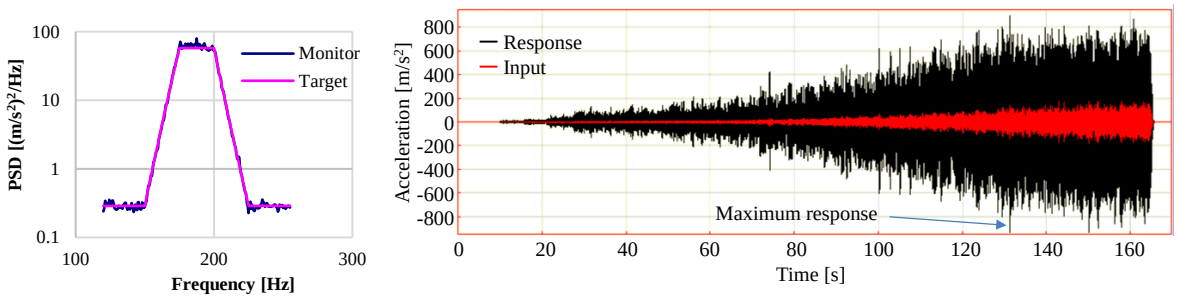

(a) PSD of input wave (b) Time history acceleration waveform of input and response

Figure 3 Waveform of excitation experiment

Experimental results

The response acceleration at the top of the scale-model cylindrical tank with low bottom stiffness is shown in Figure 3(b). While the input acceleration increases gradually with time, the time waveform of the response acceleration does not increase in amplitude after 132 seconds or later. It can be seen that the scale-model cylindrical tank responds nonlinearly when the acceleration is large. The maximum response acceleration was 937 m/s^2 at 132 seconds, and the input acceleration was 146 m/s^2 at that time.

The post-buckling deformed shape of the scale-model cylindrical tank with low bottom stiffness is shown in Figure 4. Here, the relationship between the direction of excitation and the orientation of the scale-model cylindrical tank is defined. The direction of excitation is 0 – 180°, with the excitation coil side at an orientation of 180°. 0° is the front, 90° is the right side facing the front, and 270° is the left side. This definition is the same as for a general compass. The scale-model cylindrical tanks were subjected to elephant-foot buckling at 180°, and the cylindrical plates were cracked longitudinally at the location where elephant-foot buckling occurred. This damage behaviour is consistent with the elephant-foot buckling that is expected to occur in large cylindrical tanks.

The post-buckling deformed shape of the scale-model cylindrical tank with high bottom stiffness is shown in Figure 5. Shear buckling occurred near the 270° base, and the cylindrical body plate was torn in the diagonal direction. On the other hand, the deformation at 0–180° was minor. This deformation shape is different from that of elephant-foot buckling, which is expected to occur in large tanks. The measured acceleration of the scale-model cylindrical tank with high bottom stiffness was not different from that of the scale-model cylindrical tank with low bottom stiffness, so it is not presented here.

These results suggest that when elephant-foot buckling occurs on a tank, the deformation of the bottom plate affects the buckling behaviour. It is estimated that the low bottom stiffness is one of the conditions that allow low-height tanks to undergo elephant-foot buckling.

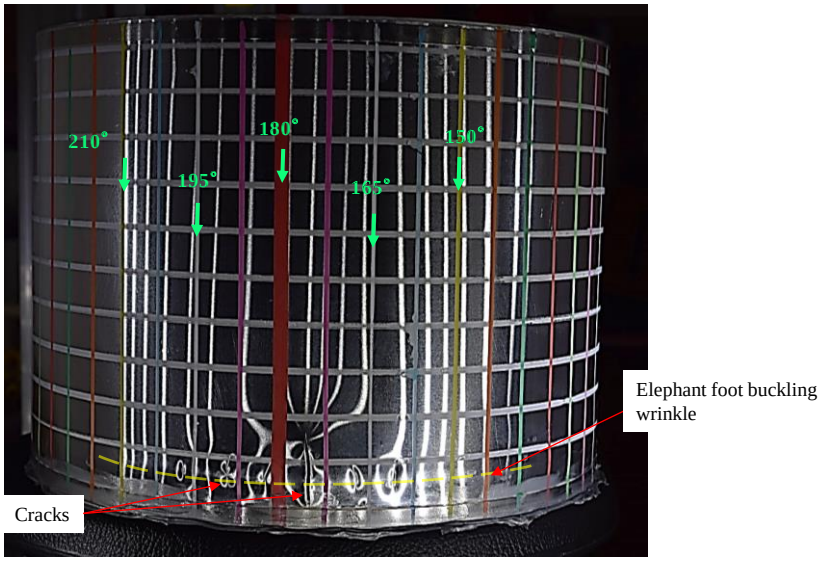

Figure 4 Deformation of scale-model cylindrical tank with low bottom stiffness after experiment

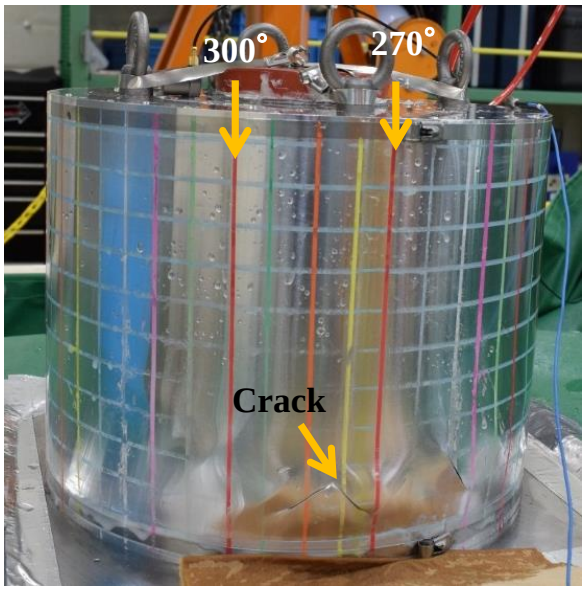

Figure 5 Deformation of scale-model cylindrical tank with high bottom stiffness after experiment

FSI ANALYSIS

In the work reported in this paper, FSI analysis using the implicit method was conducted for the experimental results of elephant-foot buckling. In this experiment, the scale-model cylindrical tank with low bottom stiffness was subjected to elephant-foot buckling, so the analytical model was developed for the scale-model cylindrical tank with low bottom stiffness.

In the weakly coupled FSI analysis applied in this study, the wall displacement obtained in the structural analysis is given to the fluid analysis, and the wall pressure obtained in the fluid analysis is returned to the structural analysis. MSC Marc® (MSC, 2021), which can analyse dynamic nonlinear

behaviours in an implicit method, was applied as the structural analysis solver, and scFLOW© (MSC, 2021), which can analyse dynamic behaviours of liquid surface in an implicit method, was applied as the fluid analysis solver. MSC-Cosim (MSC, 2020) was applied for the coupled process of the two solvers, and the stability of the analysis was ensured by the convergence calculation in the coupled process.

Structural analysis model

The element division and boundary conditions of the structural analysis model are shown in Figure 6. The cylindrical plate was divided into 160 elements in the circumferential direction, and a 6 mm square element division with an aspect ratio of 1 was applied in the height direction. The five nodes at the bottom of the model were fixed, and boundary conditions were set to load the horizontal acceleration waveform on the fixed points. The material properties of the analytical model are presented in the following sentences. The bottom plate was modeled as an elastic material to allow for deformation. The material of the bottom was set to be an elastic material with a Young's modulus of 200 GPa and a density of 7.8×10^3 kg/m^3. The tank body plate, which was repeatedly subjected to large deformation by buckling, was made of an elasto-plastic material with Young's modulus of 70 GPa and yield stress of 70 MPa. The behaviour of this material after yielding was determined by a composite hardening law based on the stress-strain relationship of the tensile experiment of a thin aluminium sheet shown in Figure 2. The material of the aluminium plate at the top of the scale-model cylindrical tank plate was modeled as an elastic material with a Young's modulus of 70 GPa. The density of the aluminium part was set to 2.7×10^3 kg/m^3.

When a real structure is excited in its natural vibration mode, various energy dissipation effects are exerted to produce damping effects, which determine the response multiplier of the natural vibration mode. Since it is difficult to simulate the real energy dissipation in FEM analysis, Rayleigh damping is modeled to demonstrate the damping effect numerically. The Rayleigh damping is separated into mass-proportional damping and stiffness-proportional damping terms, each of which has its own frequency characteristics. In general, the two damping effects are combined in seismic analysis, and the damping model is set up so that the damping effect is as close as possible to the target damping ratio around the targeted frequency.

In the work reported in this paper, the total damping ratio was set to be 2.5% at the natural frequency of 200 Hz for the overturning mode. This damping ratio was set to reproduce the experimental results. The frequency response of the Rayleigh damping is shown in Figure 8. This controllability of the damping ratio is important for future design evaluations based on analysis. It will be important to establish a method for setting and confirming the damping ratio when conducting analysis for design evaluation, where conservatism is required.

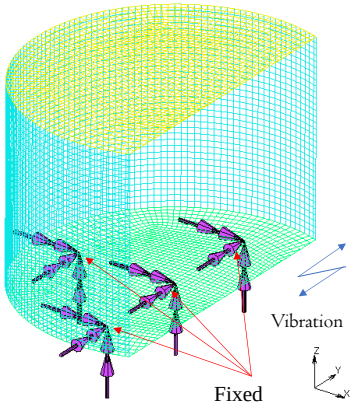

Figure 6 Structural analysis model

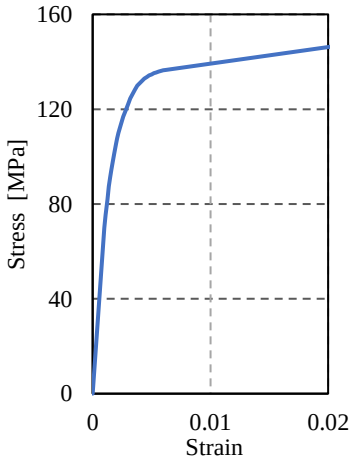

Figure 7 Stress-strain relationship of tank body plate

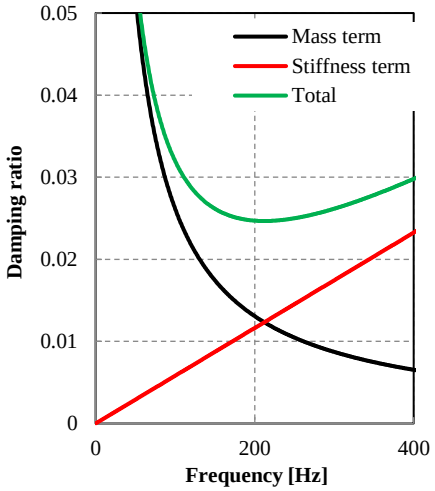

Figure 8 Variation of Rayleigh damping ratio with frequency

Fluid Analysis Model

In this paper, the object of fluid analysis consists of water and air, and it has a free surface. The dimensions of the space are as shown in the structural analysis model. The position of the free water surface was defined to be 180 mm from the bottom surface. For the elemental divide of the fluid analysis model, the state of the model cut plane is shown in Figure 9. Since the fluid near the centre of the model does not flow much, the centre of the model was roughly divided into elements, and the area near the wall was divided so that the length of the elements was approximately equal to the length of the structural analysis elements. In the area near the wall, a prismatic ray mesh was set up to place thin plate fluid elements in the direction normal to the wall.

The physical properties of the analytical model are explained in the following sentences. Water is an incompressible fluid, and its density is set to 998 kg/m^3. Air is a compressible fluid with a constant compressibility, and its density is set to 1.18 kg/m^3. The interface between the two layers of water and air was modeled using the Volume of Fluid method (MSC, 2021). A laminar flow model was used for the flow field to eliminate additional damping. However, near the wall, compressibility was set, which is characterized by being effective only during the convergence calculation of the coupled analysis. The fluid domain with this setting is called the cushion domain (MSC, 2021). scFLOW© uses this compressibility to speed up and stabilize convergence calculations. The reason why a prismatic ray mesh is used is to improve the stability of the cushion region, even though the fluid hardly flows.

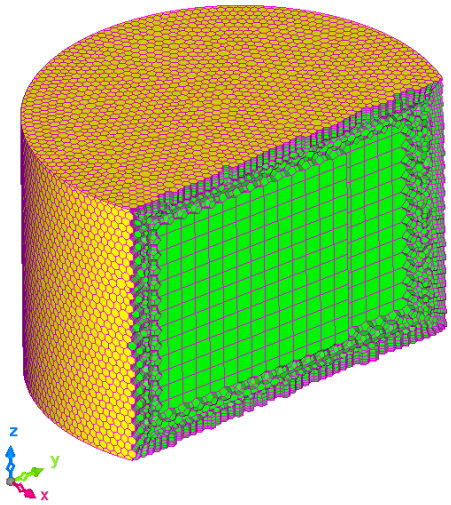

Figure 9 Fluid analysis model

FSI Analysis Result for Setting Confirmation

In excitation analysis, it is important that the natural frequencies and damping settings of the analytical model are appropriate. In FSI analysis, the natural frequency of the analysis model cannot be obtained by linear perturbation calculation. In FSI analysis, it is also necessary to check the effectiveness of the damping setting in the structural analysis solver.

In the work reported in this paper, a free vibration analysis was conducted to confirm the natural frequencies and damping ratios of the overturning mode in the FSI analysis. The natural frequency was derived based on the period of the displacement at the top of the scale-model cylindrical tank, and the damping ratio was calculated based on the reduction ratio of the amplitude of the displacement at the top of the scale-model cylindrical tank. The time history waveform of the displacement of the top of the scale-model cylindrical tank was shown in Figure 10 as a result of the FSI analysis for setting confirmation. The natural frequency calculated from the analysis results was 243 Hz, and the damping ratio was 2.51%.

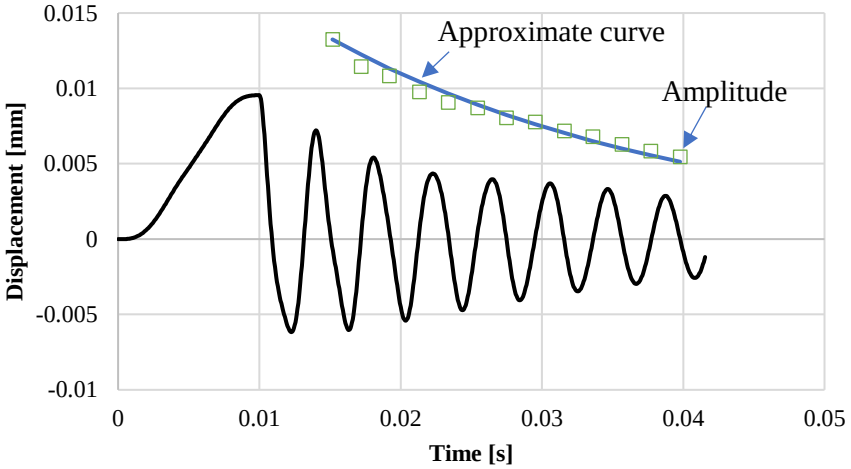

Figure 10 Time history waveform of the displacement of the top of the scale-model cylindrical tank during free vibration

FSI Analysis Result of the Excitation Experiment

The following sentences present the results of the FSI analysis simulating the excitation experiment with the scale-model cylindrical tank. The time waveforms of the input and response accelerations are shown together in Figure 11. In this paper, the maximum response acceleration is defined as the response acceleration during buckling. The analytical result of the response acceleration during buckling is 877 m/s^2, and the error from the experiment result (934 m/s^2) is about 6%. The time history waveform of the input acceleration in analysis was extracted from the time history waveform of the input acceleration in the experiment shown in Figure 3 around the time when the maximum response acceleration was observed.

A representative deformation diagram from the analysis results at time 0.07 s is shown in Figure 12. The equivalent plastic strain on the neutral surface is displayed as a contour. From this deformation diagram, it can be seen that there is an outward swelling near the bottom of the compression side of the bending deformation and plasticization of the neutral plane at the location of the deformation. The response acceleration during buckling and the shape of the deformation after buckling were in good agreement with the experiment results, confirming the validity of the analysis method.

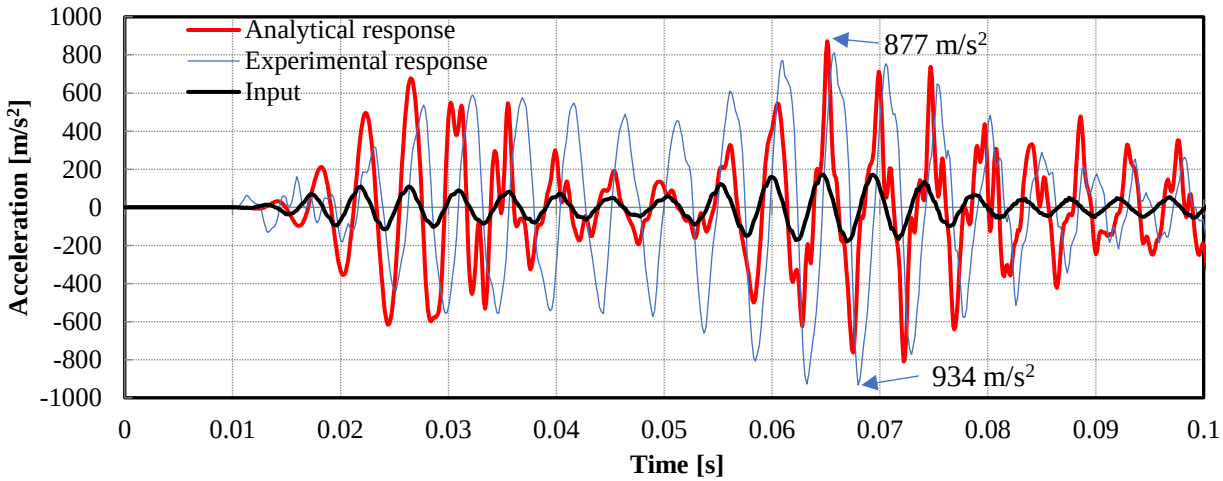

Figure 11 Comparison of analytical and experimental results of the acceleration waveform.

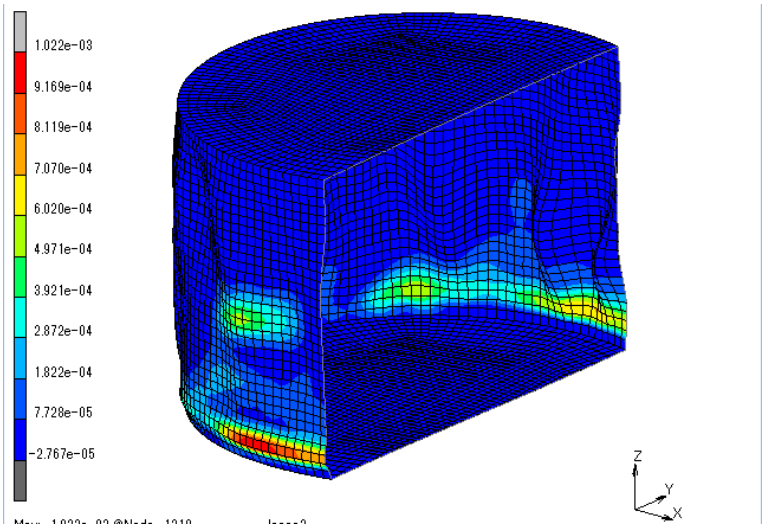

Figure 12 Deformation diagram at the time of occurrence of elephant-foot buckling displaying contour of equivalent plastic strain

CONCLUSION

In this paper an experiment using scale-model cylindrical tanks and a simulation analysis using fluid-structure interaction (FSI) are presented for the phenomenon of earthquake-induced elephant-foot buckling of a large cylindrical vertical flat-bottomed fixed tank containing water. The buckling behaviour observed in the excitation experiments using the scale-model tanks was the same as that expected in a large actual tank. The FSI analysis simulated the scaled-down experiment with high accuracy, and the following conclusions were obtained.

1. When elephant-foot buckling occurs in a cylindrical tank whose height is the same as the radius of the tank, the stiffness of the bottom of the tank affects the damage behaviour. It is estimated that low bottom stiffness is one of the conditions necessary for a low-height tank to undergo elephant-foot buckling.
2. As a result of the simulation by FSI analysis for the experiment with the scale-model cylindrical tank, the analytical model was able to achieve elephant-foot buckling with a shape similar to that of the buckling obtained in the experiment. The error between the maximum response accelerations of the analytical results and the experimental results was only about 6%, indicating that the experiment was simulated with high accuracy.

In summary, it is now possible to accurately understand the seismic behaviour of cylindrical tanks, including the effects of fluid interaction and plastic deformation associated with buckling. Using this analysis technique as an evaluation method for actual tanks will improve the accuracy of the evaluation, which is expected to contribute to the rationalization of the evaluation and the improvement of the reliability of nuclear power plants.

REFERENCES

Electric Power Research Institute (EPRI) ed. (1990), *"Loma Prieta Earthquake Reconnaissance Report, Earthquake Spectra"*, Supplement to Volume 6

Akira Maekawa (2009), *"Dynamic Buckling Analysis of Cylindrical Water Storage Tanks"*, PVP2009-77083

MSC Software Ltd., (2021), *"Marc®: User Inf Manual: Marc® 2021.1 Volume A"*

MSC Software Ltd., (2021), *"scFLOW© 2021 Software Cradle: Analysis User's Manual: Version 2021"*

MSC Software Ltd., (2020), *"MSC CoSim: MSC CoSim 2020 User's Guide: Version 2020"*